J. Biochem. **123**, 324-331 (1998)

Ca^{2+}-Induced Distance Change between Points on Actin and Troponin in Skeletal Muscle Thin Filaments Estimated by Fluorescence Energy Transfer Spectroscopy

Masao Miki,*,[1] Tomoyoshi Kobayashi,[†] Hiroyuki Kimura,* Akihiko Hagiwara,* Hong Hai,* and Yuichiro Maéda[†]

**Department of Applied Chemistry and Biotechnology, Fukui University, 3-9-1 Bunkyo, Fukui 910;* [†]*International Institute for Advanced Research, Matsushita Electric Industrial Co., Ltd., 3-4 Hikaridai, Seika 619-02*

Received for publication, September 16, 1997

Fluorescence resonance energy transfer spectroscopy has been used to study the spatial relationships between probes attached to actin and troponin in the reconstituted skeletal muscle thin filament in the presence and absence of Ca^{2+} ions. Gln-41 and the nucleotide-binding site of actin were selectively labeled with the acceptor probe: fluorescein cadaverine and 2′(or 3′)-*O*-(2,4,6-trinitrophenyl)adenosine 5′-diphosphate (TNP-ADP), respectively. Troponin was selectively labeled at positions 9 or 133 of troponin-I and 98 of troponin-C with a donor probe; 5-(2-iodoacetylaminoethyl)aminonaphthalene 1-sulfonic acid (IAEDANS). The distances between probes attached to position 133 of TnI and Gln-41 or the nucleotide site of actin were determined to be 51.6±1.2 and 42.7±0.9 Å respectively in the presence of Ca^{2+}, and these distances decreased by 11.5 and 9.3 Å respectively in the absence of Ca^{2+} ions. The distances between the probes attached to position 9 of TnI and Gln-41 or the nucleotide site of actin were determined to be 59.1±2.0 or 49.3±1.5 Å respectively in the presence of Ca^{2+}, and the distances decreased by 5.3 or 3.7 Å in the absence of Ca^{2+}. The distances between probes attached to position 98 of TnC and Gln-41 or the nucleotide site of actin were determined to be 55.1±1.7 and 57±5 Å in the presence of Ca^{2+} and the distances increased slightly by ~1 Å in the absence of Ca^{2+}. The results suggest that the C-terminal domain of troponin I moves to the outer domain of actin during inhibition, while the C-terminal domain of TnC does not move much.

Key words: actin, Ca^{2+}-induced conformational change, fluorescence resonance energy transfer, skeletal muscle thin filaments, troponin.

In striated muscle, the interaction of myosin with actin is regulated by tropomyosin (Tm) and troponin (Tn) on the actin filament in response to a change from approximately 10^{-7} to 10^{-5} M in Ca^{2+} concentration (*1*). Tn serves as a molecular switch in regulation of skeletal muscle contraction. Tn is a complex of three proteins: TnC, which binds Ca^{2+}; TnI, which inhibits actomyosin ATPase activity; and TnT, which binds Tm. The binding of Ca^{2+} to TnC induces a conformational change in Tn, which is propagated along the actin filament by Tm. Numerous studies have characterized the interaction between the thin filament proteins to deduce how the Ca^{2+}-triggering signal is propagated from TnC to the rest of the thin filament. [For reviews, see Zot and Potter (*2*) and Farah and Reinach (*3*)]. X-ray diffraction studies revealed that TnC is dumbbell-shaped, with two similar domains separated by a long, central helix (*4*). The N-terminal domain contains two low-affinity metal-binding sites which bind Ca^{2+} specifically and are responsible for the regulation of muscle contraction, while the C-terminal domain contains two high-affinity sites which are occupied by Mg^{2+} under physiological conditions. It was demonstrated that the N-terminal domain of TnI interacts strongly with the C-terminal domain of TnC, irrespective of the calcium concentration (in the presence of magnesium), while the C-terminal plus inhibitory domain of TnI and the N-terminal domain of TnC interacts in a calcium-dependent manner (*5*). The TnI-TnC complex binds to the C- terminal region of TnT to form a globular portion of Tn. TnT is an elongated protein (*6*) which lies extended along the C-terminal third of the Tm coiled coil from Cys-190 to the C-terminus of Tm, where it overlaps the NH_2 terminus of the adjacent Tm (*2*).

Fluorescence resonance energy transfer (FRET) has been extensively used for studying the spatial relationships between residues on muscle proteins [see reviews: dos Remedios *et al.* (*7*) and Miki *et al.* (*8*)]. This method is especially valuable for detecting a small conformational change, since the transfer efficiency is a function of the inverse of the sixth power of the distance between probes. Using this method, several attempts have been made to detect conformational changes of thin filaments in response

[1] To whom correspondence should be addressed. Tel: +81-776-27-8786, Fax: +81-776-27-8747, E-mail: masao@acbio.fukui-u.ac.jp

Abbreviations: DTT, dithiothreitol; EGTA, ethylene glycol-bis(2-aminoethyl ether)-*N,N,N′,N′*-tetraacetic acid; FLC, fluorescein cadaverine; FRET, fluorescence resonance energy transfer; IAEDANS, 5-(2-iodoacetylaminoethyl)aminonaphthalene 1-sulfonic acid; TNP-ADP, 2′(or 3′)-*O*-(2,4,6-trinitrophenyl)adenosine 5′-diphosphate; Tm, tropomyosin; Tn, troponin.

to a change in Ca^{2+} concentration in order to understand the switching mechanism of Tn. The distance between probes on Cys-133 of TnI and Cys-374 or Lys-61 on actin were increased significantly by Ca^{2+} binding to the regulatory sites of TnC (*9, 10*). The time rate of this conformational change observed by a stopped-flow fluorometry was fast enough to allow this TnI movement on actin filaments to be directly involved in activation of muscle contraction (*11*). Spatial relationships between Tn subunits in Tn were also studied by FRET (*12, 13*).

Cys-133 on TnI is located on the C-terminal region. In the present study, a mutant TnI was expressed, in which the natural cysteines (48, 64, and 133) were replaced with Ala or Ser and a single Cys residue was introduced at position 9 on the N-terminal region. Cys-98 on TnC is a natural single cysteine and is located on the helix region close to the C-terminal domain. Thus, Cys-133 or Cys-9 of TnI, and Cys-98 of TnC were selectively labeled with a fluorescence resonance donor molecule, IAEDANS. On the other hand, Gln-41 and the nucleotide-binding site on actin were labeled with the acceptors fluorescein cadaverine and TNP-ADP, respectively. According to the atomic structure of actin (*14*), actin consists of two well-separated domains. Subdomains 1 and 2 constitute the small domain, whereas subdomains 3 and 4 comprise the large domain. The nucleotide-binding site is located at the cleft region between the two domains, and Gln-41 is located on subdomain 2. The interactions between TnI, TnC, and actin are essential for the Ca^{2+}-dependent regulation of skeletal muscle contraction. In order to understand the function of Tn as a molecular switch, FRET between these probes on Tn and actin was measured in the presence and absence of Ca^{2+}.

MATERIALS AND METHODS

Reagents—Phalloidin from *Amanita phalloides* was purchased from Boehringer Mannheim Biochemica. 2′(or 3′)-*O*-(2,4,6-trinitrophenyl)adenosine 5′-triphosphate (TNP-ATP) was synthesized according to the method of Hiratsuka and Uchida (*23*). IAEDANS and fluorescein cadaverine (FLC) were purchased from Molecular Probes. BCA protein assay reagent was from Pierce Chemicals. CM-Toyopearl 650 M was from Toso, Tokyo. All other chemicals were analytical grade.

Protein Preparations—Actin, S1, tropomyosin, and troponin from rabbit skeletal muscle were prepared as described in a previous report (*10*). Troponin subunits were prepared according to the method of Ojima and Nishita (*15*) by using CM-Toyopearl. Mutant TnI (Ala-9-Cys, Cys-48-Ala, Cys-64-Ala, Cys-133-Ser, Trp-161-Phe) was expressed and purified as previously reported (*13*). Microbial transglutaminase was a generous gift from Food Research and Development Laboratories, Ajinomoto. In contrast to transglutaminase from guinea pigs, this enzyme does not require Ca^{2+} for its activity (*16, 17*). Protein concentrations were determined from absorbance measurements, using absorption coefficients of $A_{290}=0.63$ $(mg/ml)^{-1}\cdot cm^{-1}$ for G-actin (*18*), and $A_{280}=0.75$ for S1 (*19*), 0.33 for tropomyosin (*20*), and 0.45 for troponin (*21*), 0.458 for TnT, 0.372 for TnI, 0.18 for TnC (*22*), and 0.122 $(mg/ml)^{-1}\cdot cm^{-1}$ for mutant TnI. Concentrations of labeled proteins and transglutaminase were measured with the Pierce BCA protein assay reagent. Relative molecular masses of 42,000 for actin, 115,000 for S1, 66,000 for tropomyosin, 69,000 for troponin, and 38,000 for microbial transglutaminase were used.

Labeling of Proteins—Labeling of actin with TNP-ADP. F-actin pellet was dissolved in 60 mM KCl and 10 mM Tris-HCl (pH 8.0), and the solution was recentrifuged to remove free ATP or ADP, since the binding affinity of TNP-ATP is significantly smaller than those of ATP and ADP. The F-actin pellet was dissolved in 1 mM Tris-HCl (pH 8.0) and 0.1 mM $CaCl_2$. The solution was sonicated on ice for up to 20 s using a Tomy UD-201 sonicator. Then 1 mM TNP-ATP was immediately added and the solution was sonicated again. A 1/10 volume of Dowex-1 was added, and after 5 min of incubation, the resin was removed by filtration. The cycle of addition of TNP-ATP, sonication and Dowex-1 treatment was repeated once. Finally, 1 mM TNP-ATP was added to the solution and incubated for 30 min on ice. TNP-ATP-G-actin thus obtained was polymerized into TNP-ADP-F-actin in 60 mM KCl, 2 mM $MgCl_2$, and 10 mM Tris-HCl (pH 8.0). The sample was centrifuged and the pellet was redissolved in the same buffer solution and recentrifuged until all free TNP-ATP in the solution was removed. Twofold molar excess of phalloidin was added to TNP-ADP-F-actin in order to prevent the depolymerization of TNP-ADP-F-actin. The concentration of TNP-ADP bound to actin was determined from optical absorbance measurements by use of a molar extinction coefficient of 26,400 $M^{-1}\cdot cm^{-1}$ at 408 nm (*23*). Typically, the labeling ratio was 0.6 ± 0.1.

Labeling of actin at Gln-41 with fluorescein cadaverin (FLC) was carried out according to the method of Takashi (*24*) by using microbial transglutaminase instead of that from guinea pigs. G-actin (50 μM) was incubated for 20 h at 4°C with a fivefold molar excess of FLC in 5 mM Tris-HCl (pH 8.0), 0.5 mM ATP, 1 mM DTT, 1 mM NaN_3, and 1 μM transglutaminase. The actin was polymerized in 50 mM NaCl and 2 mM $MgCl_2$ and centrifuged at $100,000\times g$ for 90 min. The pellet was homogenized in 0.1 M NaCl, 2 mM $MgCl_2$, and 0.5 mM DTT and recentrifuged to remove free FLC. The labeled actin pellet was suspended in 2 mM Tris-HCl (pH 8.0), 0.1 mM ATP, 0.1 mM $CaCl_2$, and 0.25 mM DTT and dialyzed against the same buffer solution. The amount of FLC bound to actin was determined by using the extinction coefficient of 75,500 $M^{-1}\cdot cm^{-1}$ at 493 nm (*25*). The labeling ratio was 0.71.

Labeling of Cys-133 of TnI with IAEDANS was carried out as previously reported (*10*). The labeling ratio of IAEDANS to troponin was 0.6. Labeling of Cys-9 in a mutant TnI was carried out by mixing with tenfold molar excess of IAEDANS in 0.4 M KCl and 20 mM phosphate buffer (pH 7.0) for 24 h at 4°C. The reaction was terminated by the addition of 1.0 mM DTT, and the sample solution was dialyzed against 5 mM phosphate buffer (pH 7.0) and 0.4 M KCl exhaustively to remove free IAEDANS. The labeling ratio was 0.48. Labeling of Cys-98 of TnC was carried out by mixing with fivefold molar excess of IAEDANS in 0.1 M NaCl, 1 mM EDTA, and 5 mM Hepes buffer (pH 7.0) at 4°C for 2 h. The reaction was terminated by the addition of 1.0 mM DTT, and the sample solution was dialyzed exhaustively against 5 mM Hepes buffer (pH 7.0). The labeling ratio was 0.43.

Reconstitution of the ternary Tn complex was carried out

according to Farah *et al.* (*5*). Labeled TnC or mutant TnI was complexed with TnT and TnI or TnC by placing equimolar amounts of each protein together in 4.6 M urea, 25 mM Tris-HCl (pH 8.0), 1 M KCl, 0.5 mM $CaCl_2$, 10 mM 2-mercaptoethanol, and 1 mM NaN_3, then dialyzing the mixture successively against 4.6, 2, and 0 M urea in 1 M KCl, 50 mM Tris-HCl (pH 8.0) with 50 μM $CaCl_2$. Then the mixture was successively dialyzed against 1 and 0.1 M KCl in 20 mM Tris-Maleate buffer (pH 7.0), 50 μM $CaCl_2$, 10 mM 2-mercaptoethanol, and 1 mM NaN_3, and finally against 20 mM Tris-Maleate (pH 7.0), 6.5 mM KCl, 3.5 mM $MgCl_2$, 50 μM $CaCl_2$, 2 mM DTT, and 1 mM NaN_3. The sample solution was centrifuged at 500,000 $\times g$ for 10 min to remove insoluble materials, since TnI and TnT alone are insoluble at low ionic strengths. The Tn complex was precipitated by centrifugation with 60% saturated ammonium sulfate at 10,000 $\times g$ for 20 min in order to separate it from free TnC. The pellet was dissolved in 2 mM Tris-HCl (pH 8.0) and dialyzed exhaustively against the same buffer solution.

Spectroscopic Measurements—Absorption was measured with a Hitachi U2000 spectrophotometer. Steady-state fluorescence was measured with a Hitachi 850 fluorometer. Sample cells were placed in a thermostated cell holder. Steady-state fluorescence polarization measurements were carried out in the presence of various concentrations of sucrose (0, 10, 20, 30, and 40% w/w) at 20°C to measure the limiting anisotropy.

Fluorescence Resonance Energy Transfer—The efficiency, E, of resonance energy transfer between probes was determined by measuring the fluorescence intensity of the donor both in the presence (F_{DA}) and absence (F_{D0}) of the acceptor as given by

$$E = 1 - F_{DA}/F_{D0} \quad (1)$$

From the absorption of the samples at the excitation (A_{ex}) and emission (A_{em}) wavelengths, the decrease of the fluorescence intensity due to inner filter effects was corrected, using Eq. 2 (*26*).

$$F_{corr} = F_{obs} \times 10^{(A_{ex}+A_{em})/2} \quad (2)$$

According to Förster's theory [see reviews: Fairclough and Cantor (*27*) and Lakowicz (*26*)], the efficiency is related to the distance (R) between probes and Förster's critical distance (R_0) at which the transfer efficiency is equal to 50% by

$$E = R_0^6/(R_0^6 + R^6) \quad (3)$$

R_0 can be obtained (in Å) by

$$R_0^6 = (8.79 \times 10^{-5}) n^{-4} \kappa^2 Q_0 J \quad (4)$$

where n is the refractive index of the medium, taken to be 1.4; κ^2 is the orientation factor; Q_0 is the quantum yield of the donor in the absence of the acceptor; and J is the spectral overlap integral (in $M^{-1} \cdot cm^{-1} \cdot nm^4$) between the donor emission $F_D(\lambda)$ and acceptor absorption $\varepsilon_A(\lambda)$ spectra defined by

$$J = \int F_D(\lambda) \varepsilon_A(\lambda) \lambda^4 d\lambda / \int F_D(\lambda) d\lambda \quad (5)$$

The quantum yield was determined by comparing the integrated corrected fluorescence spectrum with that of quinine sulfate in 0.1 N H_2SO_4, whose quantum yield was taken to be 0.70 (*28*). κ^2 was taken as 2/3 for calculation of distances, and the maximum and minimum values of κ^2 were estimated by the method of Dale *et al.* (*29*).

Other Methods—SDS-PAGE was carried out according to Laemmli (*30*). ATPase activity was measured by the method of Tausky and Shorr (*31*). The biological activity of the labeled troponin was assayed by determining the Ca^{2+}-dependent regulation of actoS1 ATPase activity in a fully reconstituted system. Measurements were performed at 25°C in 10 mM KCl, 2.5 mM $MgCl_2$, 5 mM ATP, 50 mM Tris-HCl (pH 8.0), and 50 μM $CaCl_2$ (+Ca state) or 1 mM EGTA (−Ca state). Protein concentrations were: 1 mg/ml F-actin, 0.25 mg/ml Tm, 0.25 mg/ml Tn, and 0.06 mg/ml S1.

RESULTS

In this work, the AEDANS moiety bound to Cys-133 of TnI, Cys-9 of a mutant TnI or Cys-98 of TnC was used as the energy-transfer donor, while FLC or TNP-ADP bound to actin was used as the energy-transfer acceptor. The absorption spectra of FLC and TNP-ADP bound to actin overlap well with the fluorescence emission spectrum of AEDANS bound to Tn (Cys-9 and Cys-133 of TnI, and Cys-98 of TnC). The Tn complex in which the TnI subunit was labeled at Cys-133 with AEDANS regulated the acto-S1 ATPase activity in response to changes in Ca^{2+} concentration as effectively as non-labeled Tn, in agreement with the previous report (*10*). The reconstituted Tn complex in which the mutant TnI was labeled at Cys-9 with AEDANS, or in which TnC was labeled at Cys-98 with AEDANS regulated the acto-S1 ATPase activity as effectively as unlabeled Tn, in agreement with the previous report (*13, 32*).

FRET between Cys-133 on TnI and the Nucleotide-Binding Site or Gln-41 on Actin in a Reconstituted Thin Filament—The overlap integral J was calculated to be 7.61×10^{14} $M^{-1} \cdot cm^{-1} \cdot nm^4$ for AEDANS-TNP-ADP and 18.67×10^{14} $M^{-1} \cdot cm^{-1} \cdot nm^4$ for AEDANS-FLC. By taking $n = 1.4$, $\kappa^2 = 2/3$, and $Q_0 = 0.31$, the Förster's critical distance R_0 was calculated to be 39.1 Å for AEDANS-TNP-ADP and 45.5 Å for AEDANS-FLC.

The fluorescence spectra of AEDANS bound to Cys-133 of TnI on the reconstituted thin filament in the absence (curves 1 and 2 in Fig. 1) and presence (curves 3 and 4 in Fig. 1) of acceptor (TNP-ADP) were measured in 30 mM KCl, 2 mM $MgCl_2$, 20 mM Tris-HCl (pH 7.6), 1 mM NaN_3 (buffer F) and 50 μM $CaCl_2$ (+Ca state: 1 and 3) or 1 mM EGTA (−Ca state: 2 and 4). The molar ratio of actin/Tm/Tn was 7:1:1. The excitation wavelength was 340 nm. Under the present experimental conditions, the fluorescence from TNP-ADP was negligibly small in comparison with that from AEDANS (curve 5 in Fig. 1). Figure 1 shows that the donor fluorescence (AEDANS) was strongly quenched in the presence of acceptor (TNP-ADP) owing to energy transfer and that the extent of the quenching was higher for −Ca state than for +Ca state.

To obtain more quantitative data for the transfer efficiency, the ratio of donor fluorescence quenching was measured by titrating AEDANS-Tn/Tm with TNP-ADP-F-actin in the presence of Ca^{2+} (buffer F + 50 μM $CaCl_2$) and absence of Ca^{2+} (buffer F + 1 mM EGTA). The fluorescence intensity of AEDANS-Tn was measured at 490 nm. For the correction of the fluorescence intensity change of

AEDANS-Tn/Tm upon binding to actin filaments, the same amount of non-labeled F-actin was added to the AEDANS-Tn/Tm solution, and the ratio of those fluorescence intensities was taken. The apparent decrease of the fluorescence intensity due to the inner filter effects by the absorbance of TNP-ADP-F-actin was corrected according to Eq. 2. The fluorescence ratio decreased in the range of the actin/Tn molar ratio up to 7 and became almost constant in the range over 7 (Fig. 2). The results suggest that the energy transfer occurs through a specific interaction between actin and troponin. Thus, from the saturated points, the apparent transfer efficiencies were taken to be 0.25 ± 0.02 in +Ca state and 0.48 ± 0.03 in −Ca state. Taking into account the labeling ratio of TNP-ADP to actin being 0.67, the transfer efficiencies were calculated to be 0.37 ± 0.03 in +Ca state and 0.72 ± 0.04 in −Ca state. These efficiencies correspond to the distances of 42.7 ± 0.9 and 33.4 ± 1.2 Å respectively, assuming that the energy transfer occurs between a single donor and a single acceptor.

FLC-G-actin was polymerized in 30 mM KCl, 2 mM $MgCl_2$, 20 mM Tris-HCl (pH 7.6), 0.1 mM ATP, and 1 mM NaN_3 (buffer A) in the presence of twofold molar excess of phalloidin. The fluorescence spectra of (1) F-actin/Tm/AEDANS-Tn, (2) FLC-F-actin/Tm/Tn, and (3) FLC-F-actin/Tm/AEDANS-Tn were measured in buffer A+50 μM $CaCl_2$ at 20°C (Fig. 3). Excitation wavelength was 340 nm. The fluorescence intensity of FLC-F-actin/Tm/AEDANS-Tn at wavelengths shorter than 480 nm was substantially quenched compared with that of F-actin/Tm/AEDANS-Tn (in the absence of acceptor). This can be

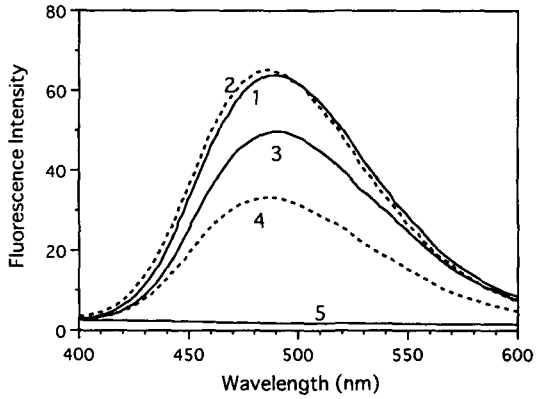

Fig. 1. **Fluorescence spectra of IAEDANS bound to Cys-133 of TnI on the reconstituted thin filament in the presence and absence of acceptor (TNP-ADP).** (1) F-actin/Tm/AEDANS-Tn/+Ca, (2) F-actin/Tm/AEDANS-Tn/−Ca, (3) TNP-ADP-F-actin/Tm/AEDANS-Tn/+Ca, (4) TNP-ADP-F-actin/Tm/AEDANS-Tn/−Ca, (5) TNP-ADP-F-actin/Tm/Tn/±Ca. Spectra were measured at 20°C in 30 mM KCl, 2 mM $MgCl_2$, 20 mM Tris-HCl (pH 7.6), 1 mM NaN_3 (buffer F), and 50 μM $CaCl_2$ (+Ca; 1, 3, and 5) or 1 mM EGTA (−Ca; 2 and 4). Concentrations of actin, Tm, and Tn were 0.2, 0.045, and 0.047 mg/ml, respectively. Excitation was 340 nm.

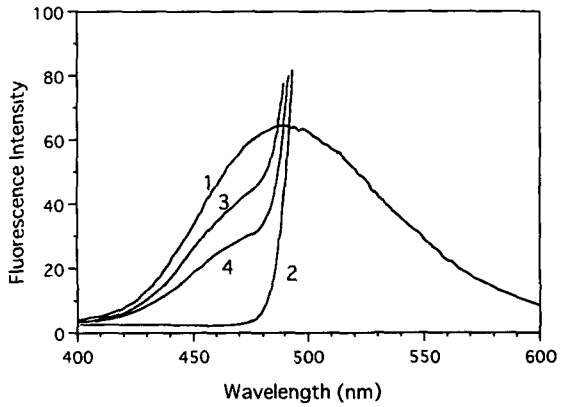

Fig. 3. **Fluorescence spectra of AEDANS bound to Cys-133 of TnI on the reconstituted thin filament in the presence and absence of acceptor (FLC).** (1) F-actin/Tm/AEDANS-Tn/+Ca, (2) FLC-F-actin/Tm/Tn/+Ca, (3) FLC-F-actin/Tm/AEDANS-Tm/+Ca, (4) FLC-F-actin/Tm/AEDANS-Tn/−Ca. Spectra were measured at 20°C in 30 mM KCl, 2 mM $MgCl_2$, 20 mM Tris-HCl (pH 7.6), 1 mM NaN_3, 0.1 mM ATP (buffer A), and 50 μM $CaCl_2$ (+Ca; 1, 2, and 3) or 1 mM EGTA (−Ca; 4). Concentrations of actin, Tm, and Tn were 0.2, 0.045, and 0.047 mg/ml, respectively. Excitation was at 340 nm. The fluorescence spectra of 2, 3, and 4 at wavelengths longer than 480 nm, which derive mainly from FLC with an emission peak at 520 nm, are omitted from the figure.

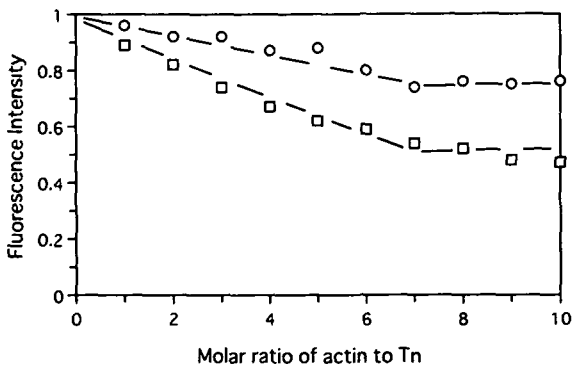

Fig. 2. **Relative fluorescence intensities of AEDANS bound to Cys-133 of TnI in the Tn-Tm complex *vs.* molar ratio of TNP-ADP-F-actin.** Values were obtained in buffer F and 50 μM $CaCl_2$ (○) or 1 mM EGTA (□) at 20°C, after correction of the inner filter effects according to Eq. 2. Concentrations of AEDANS-Tn and Tm were 0.047 and 0.045 mg/ml, respectively. Excitation was at 340 nm and emission was measured at 490 nm.

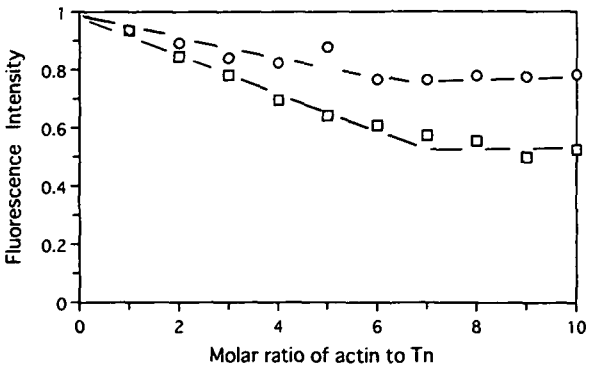

Fig. 4. **Relative fluorescence intensities of AEDANS bound to Cys-133 of TnI in the Tn-Tm complex *vs.* molar ratio of FLC-F-actin.** Values were obtained in buffer A and 50 μM $CaCl_2$ (○) or 1 mM EGTA (□) at 20°C, after correction of the inner filter effects. Concentrations of AEDANS-Tn and Tm were 0.047 and 0.045 mg/ml, respectively. Excitation was at 340 nm and emission was measured at 460 nm.

attributed mainly to the resonance energy transfer from AEDANS-Tn to FLC-F-actin. The addition of 1 mM EGTA to this sample decreased the fluorescence intensity by about 30% (curve 4 in Fig. 3), although the fluorescence intensity of F-actin/Tm/AEDANS-Tn (in the absence of acceptor) increased slightly by the addition of 1 mM EGTA (see curve 2 in Fig. 1). The results suggest that the distance between Gln-41 on actin and Cys-133 on TnI in the reconstituted thin filament decreased by the addition of EGTA. To obtain more quantitative data for the transfer efficiency, the ratio of donor quenching was measured by titrating AEDANS-Tn/Tm with FLC-F-actin in the presence and absence of $CaCl_2$ as described in the case of TNP-ADP-F-actin and AEDANS-Tn/Tm. The fluorescence intensity was measured at 460 nm, where no contribution from the fluorescence of FLC occurs (Fig. 3). After the correction of inner filter effects, the decrease of the fluorescence intensity saturated at the molar ratio of actin to Tn of 7 (Fig. 4). The apparent transfer efficiencies were determined to be 0.23 ± 0.02 in +Ca state and 0.48 ± 0.04 in −Ca state. Taking into account the labeling ratio of FLC to actin of 0.71, the transfer efficiencies were calculated to be 0.32 ± 0.03 in +Ca state and 0.68 ± 0.06 in −Ca state. These efficiencies correspond to the distances of 51.6 ± 1.2 and 40.1 ± 1.9 Å respectively, assuming that the transfer occurs between single donor and single acceptor.

FRET between Cys-9 on a Mutant TnI and the Nucleotide-Binding Site on Actin in a Reconstituted Thin Filament—The fluorescence spectrum of AEDANS bound to Cys-9 of the mutant TnI in the reconstituted Tn complex was similar to that bound to Cys-133 of wild type TnI. Quantum yield of AEDANS bound to Cys-9 of the mutant TnI in the Tn complex was 0.37. R_0 was calculated to be 40.3 Å for AEDANS-TNP-ADP and 46.9 Å for AEDANS-FLC.

The ratio of donor quenching was measured by titrating AEDANS-Tn/Tm with TNP-ADP-F-actin in the presence and absence of Ca^{2+} as described in the case of Cys-133 of TnI. The ratio of donor quenching was measured at 490 nm. The apparent transfer efficiencies were 0.15 ± 0.02 in +Ca state and 0.25 ± 0.02 in −Ca state. Taking into account the labeling ratio of TNP-ADP to actin, the transfer efficiencies were calculated to be 0.23 ± 0.03 in +Ca state and 0.37 ± 0.03 in −Ca state, which correspond to the distances 49.3 ± 1.5 and 44.0 ± 1.0 Å, respectively. Similar experiments were performed using FLC-F-actin as the acceptor in the presence and absence of Ca^{2+}. The ratio of donor quenching was measured at 460 nm. The apparent transfer efficiencies were 0.14 ± 0.02 in +Ca state and 0.19 ± 0.02 in −Ca state. The distances were calculated to be 59.1 ± 2.0 Å in +Ca state and 55.4 ± 1.4 Å in −Ca state.

FRET between Cys-98 of TnC and the Nucleotide-Binding Site on Actin in a Reconstituted Thin Filament—The fluorescence spectrum of AEDANS bound to Cys-98 of TnC in the Tn complex was similar to that bound to Cys-133 of TnI, except that the emission peak was blue-shifted by 10 nm in agreement with the previous report (*12*). Quantum yield of AEDANS bound to Cys-98 of TnC in the Tn complex was determined to be 0.25 in +Ca state and 0.23 in −Ca state. R_0 was calculated to be 37.7 Å/37.0 Å (+Ca/−Ca) for AEDANS-TNP-ADP and 43.9 Å/43.1 Å (+Ca/−Ca) for AEDANS-FLC.

The ratio of donor quenching was measured at 480 nm using TNP-ADP-F-actin as the acceptor in the presence and absence of Ca^{2+} as described in the case of Cys-133 of TnI. After the correction of the inner filter effects, the apparent transfer efficiencies were 0.05 ± 0.02 in +Ca and 0.04 ± 0.02 in −Ca states. The transfer efficiencies were too low for an accurate estimation of R. Taking into account the labeling ratio of TNP-ADP to actin (0.67), the distances were estimated to be 57 ± 5 Å in +Ca state and 59 ± 7 Å in −Ca state. The ratio of donor quenching was also measured using FLC-F-actin as the acceptor in the presence and absence of Ca^{2+}. The fluorescence intensity of the donor was measured at 460 nm to avoid emission from the acceptor molecule, FLC. The apparent transfer efficiencies were 0.14 ± 0.02 in +Ca state and 0.12 ± 0.02 in −Ca state. The distances were calculated to be 55.5 ± 1.7 Å in +Ca state and 56.2 ± 2.1 Å in −Ca state. In contrast to the other sites on Tn, the distance between Cys-98 of TnC and Gln-41 on actin decreased slightly upon Ca^{2+} binding.

DISCUSSION

In the present analysis of FRET data, a single donor-acceptor pair was assumed. However, the energy transfer may occur between a single donor on Tn and multiple acceptors on actin in a reconstituted thin filament. The transfer efficiency depends on the sixth power of the distance between a donor and an acceptor. When one acceptor is close to a donor and other acceptors lie at slightly greater distances, the transfer efficiency strongly depends on the distance of the closest acceptor. When two or three acceptors lie equidistant from a single donor molecule, the distance between the donor and the acceptors differs only by 12 or 20% respectively from the value calculated for a single donor-acceptor pair (*33*). Therefore, the present analysis gives a nearest-neighbor distance without a large error.

In calculation of the distances between probes, the value of 2/3 was used for the orientation factor, which corresponds to the case where both donor and acceptor molecules rotate rapidly. The upper and lower bounds of this parameter were calculated according to the method of Dale *et al.* (*29*). The limiting anisotropies of FLC bound to Gln-41 on actin and of AEDANS bound to Cys-98 on TnC in the Tn

TABLE I. **Distances between probes attached to Tn and actin in the reconstituted thin filament in the presence and absence of Ca^{2+}.**

Donor site (troponin)	Acceptor site (actin)	Efficiency (+Ca/−Ca)	R(2/3) (Å) (+Ca/−Ca)
Cys-133 of TnI	Nucleotide	$0.37\pm0.03/0.72\pm0.04$	$42.7\pm0.9/33.4\pm1.2$
	Gln-41	$0.32\pm0.03/0.68\pm0.06$	$51.6\pm1.2/40.1\pm1.9$
Cys-9 of TnI	Nucleotide	$0.23\pm0.03/0.37\pm0.03$	$49.3\pm1.5/44.0\pm1.0$
	Gln-41	$0.20\pm0.03/0.28\pm0.03$	$59.1\pm2.0/55.4\pm1.4$
Cys-98 of TnC	Nucleotide	$0.08\pm0.03/0.06\pm0.03$	57 ± 5 / 59 ± 7
	Gln-41	$0.20\pm0.03/0.17\pm0.03$	$55.1\pm1.7/56.2\pm2.1$

complex were previously reported to be 0.217 (*34*) and 0.179 (*12*), respectively, and those of AEDANS bound to Cys-133 of TnI and Cys-9 of the mutant TnI in the Tn complex were determined to be 0.205 and 0.331, respectively (this study). The fundamental anisotropies of AEDANS and FLC were previously reported to be 0.376 and 0.341, respectively (*34*). These values give a maximum error range for the critical distance (R_0) calculated by using $\kappa^2=2/3$ of ~30%, *i.e.*, the calculated range appears to be unacceptably large. However, it has been argued by several authors that the choice of 2/3 for κ^2 is not an unreasonable one due to electronic and rotational depolarization mechanisms (*7, 35*). We have pointed out that reasonable agreement was obtained between intra- and inter-molecular distances in G-actin and F-actin determined by FRET by assuming $\kappa^2=2/3$ and the distances determined by x-ray diffraction data (*8, 36*).

Previously, Tao *et al.* (*12*) reported that the binding of Ca^{2+} to TnC induces a conformational change in the Tn complex which causes a decrease in the distance between Cys-98 of TnC and Cys-133 of TnI by ~5 Å. Further, it has been reported that the distances between probes attached to Cys-133 of TnI and Lys-61 (*10*) or Cys-374 (*9*) of actin increased by 6 or ~15 Å upon Ca^{2+} binding to TnC. The distances between probes attached to Tn and actin in the reconstituted thin filament determined in the present study are summarized in Table I. The distances between probes attached to Cys-133 of TnI and Gln-41 or the nucleotide-binding site of actin increased by ~10 Å on binding of Ca^{2+} to Tn, while the distance between probes attached to Cys-9 of TnI and the residues on actin increased by ~4 Å upon binding of Ca^{2+} to Tn. On the contrary, the distance

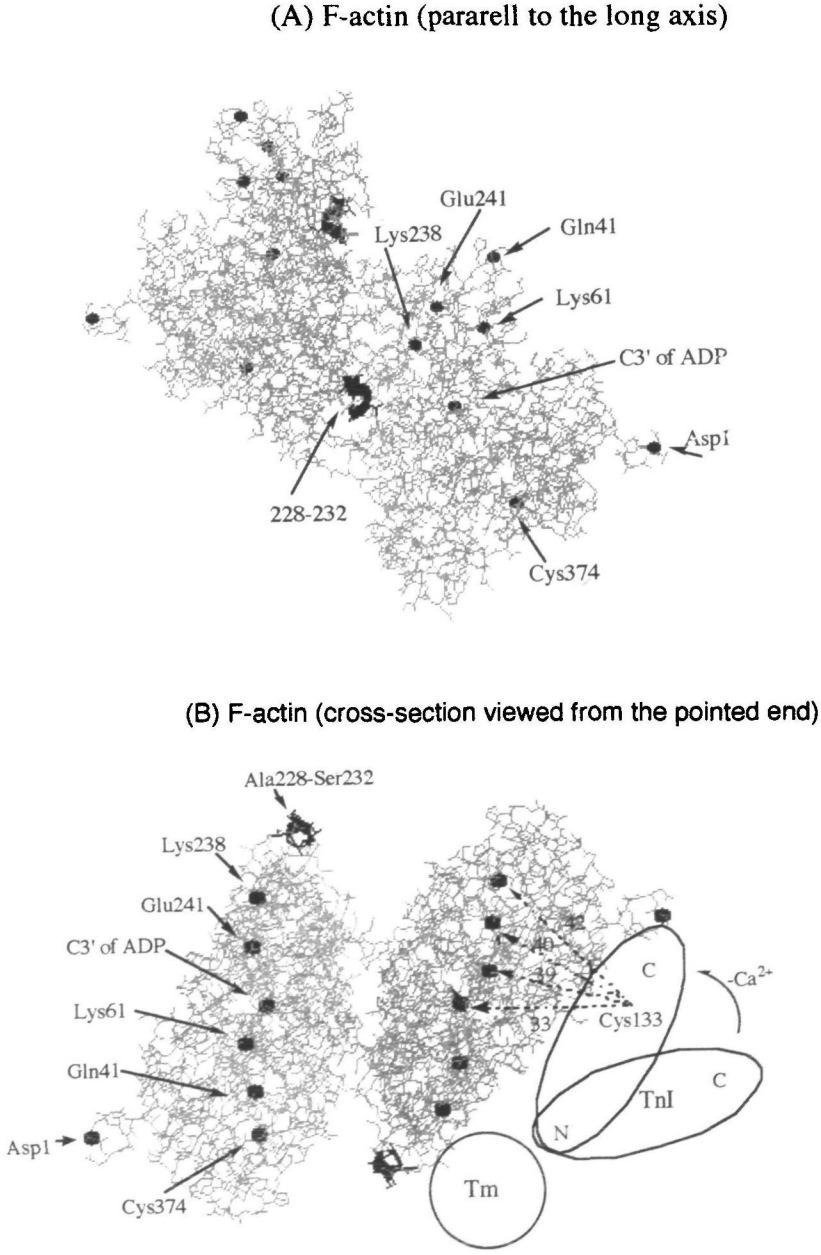

Fig. 5. **Atomic model of F-actin showing locations of residues related to the present work.** (A) view along the helix axis, (B) cross-section viewed from the pointed end. F-actin is constructed of two monomers using the atomic coordinates of Lorenz *et al.* (*38*). Cα of Asp-1, Gln-41, Lys-61, Lys-238, Glu-241, and Cys-374, and C3′ of bound ADP are shown with closed circles, and residues 228-232 are shown with ribbon structure on the wireframe model of F-actin. The software used for the figure was Rasmol by Roger Sayle. In Fig. 5B, one possible spatial relationship between TnI and actin in the presence and absence of Ca^{2+} is illustrated. The position of Tm (in the presence of Ca^{2+}) is quoted from Saeki *et al.* (*41*).

between Cys-98 of TnC and the residues on actin decreased slightly (~1 Å) on binding of Ca^{2+} to Tn. The results are in good accordance with the model of Reinach *et al.* (*37*). According to this model, the TnC/TnI dimer is organized in a structural domain (N-terminal domain of TnI and the C-terminal domain of TnC), which is responsible for the stable association of the complex to the actin filament irrespectively of the presence or absence of Ca^{2+} ions, and a regulatory domain (inhibitory and C-terminal domain of TnI and the N-terminal domain of TnC), which is responsible for the regulatory properties of the protein.

Figure 5 shows the model of F-actin (two protomers) by Lorenz *et al.* (*38*), in which Cα of several amino acid residues are indicated by closed circles. FRET measurements showed that the distances between the sites (Cys-133 or Cys-9) of TnI and the sites (Gln-41, Lys-61, Cys-374, the bound nucleotide) of actin always decreased when Ca^{2+} ions are removed from troponin. Since these sites are dispersed on the outer domain of actin, the results indicate that TnI comes closer to the outer domain of actin in the absence of Ca^{2+} ions. Grabarek and Gergely (*39*) showed that TnI has been crosslinked to F-actin near the N-terminus of actin. Using cryo-electron microscopy and image analysis, Milligan *et al.* (*40*) determined the positions of Tm on the F-actin filament in the presence of both Ca^{2+} and the myosin head, in which Tm is bound to the inner domain of actin close to the genetic helix contact. Saeki *et al.* (*41*) identified the tropomyosin-binding sites on the dictyostelium actin surface by using the method of site-directed mutagenesis. They reported that residues 228-232, 238, and 241 on actin are involved in the tropomyosin-binding site. These sites are also indicated in Fig. 5. TnI appears to protrude from the binding site on Tm toward the N-terminus of actin.

The present results indicate that Cys-133 of TnI is located closer to the outer domain of actin than Cys-9 of TnI and Cys-98 of TnC, and the distance change relative to the outer domain of actin in response to a change in Ca^{2+} concentration is larger than for Cys-9. It should be noted that in a hinge bending motion, the distance between a moving point and the hinge point does not change. Therefore, the distances between Cys-133 or Cys-9 of TnI and Cys-98 of TnC do not necessary change to the same extent as the distance changes of these residues relative to actin. In fact, the distance between Cys-133 of TnI and Cys-98 of TnC changes by -5 Å upon Ca^{2+} binding (*12*), which is much smaller than the distance change ($+15$ Å) between Cys-133 of TnI and Cys-374 of actin (*9*). During inhibition, the C-terminal and inhibitory domains of TnI decrease the affinity for the N-terminal domain of TnC (*3*) and move towards the outer domain of actin on the skeletal muscle thin filament, while the C-terminal domain of TnC does not move. TnI thus acts something like a lever arm, and the C-terminal region of TnC acts as the hinge. In Fig. 5B, the distances between Cys-133 of TnI and Gln-41, Lys-61 (*10*), Cys-374 (*9*), and the bound nucleotide of actin in the absence of Ca^{2+} are indicated (in Å unit), and one possible spatial relationship between TnI and actin in the presence and absence of Ca^{2+} is illustrated. There are many positively charged amino acid residues in the inhibitory and the C-terminal domains of TnI (in 96-178, 24 positive charges and 14 negative charges). On the other hand, the N-terminus of actin contains a string of four acidic residues (D1, E2, D3, and E4). This negative charge cluster of the actin N-terminus is crucial for the ATP-dependent actin-myosin interaction (*42, 43*). During inhibition, movement of a positively charged peptide of TnI toward the negative charge cluster of the actin N-terminus may disturb the actin-myosin interaction. This movement may be an important event in the inhibitory mechanism by the troponin-tropomyosin regulatory system.

We thank Food Research and Development Laboratories of Ajinomoto Co. for generous gift of their microbial transglutaminase, Dr. Lorenz for providing atomic coordinates of the F-actin filament over the internet, and Dr. John H. Collins for critical reading of the manuscript. We also thank Mr. Hiroyuki Kondo and Mr. Hiroshi Ishida for their technical assistance in this study.

REFERENCES

1. Ebashi, S., Endo, M., and Ohtsuki, I. (1969) Control of muscle contraction. *Q. Rev. Biophys.* **2**, 351-384
2. Zot, H.G. and Potter, J.D. (1987) Structural aspects of troponin-tropomyosin regulation of skeletal muscle contraction. *Annu. Rev. Biophys. Biophys. Chem.* **16**, 535-559
3. Farah, C.S. and Reinach, F.C. (1995) The troponin complex and regulation of muscle contraction. *FASEB J.* **9**, 755-767
4. Herzberg, O. and James, M.N.G. (1985) Structure of the calcium regulatory muscle protein troponin-C at 2.8 Å resolution. *Nature* **313**, 653-659
5. Farah, C.S., Miyamoto, C.A., Ramos, C.H.I., da Silva, A.C.R., Quaggio, R.B., Fujimori, K., Smillie, L.B., and Reinach, F.C. (1994) Structural and regulatory functions of the NH_2- and COOH-terminal regions of skeletal muscle troponin I. *J. Biol. Chem.* **269**, 5230-5240
6. Ohtsuki, I. (1979) Molecular arrangement of troponin-T in the thin filament. *J. Biochem.* **86**, 491-497
7. dos Remedios, C.G., Miki, M., and Barden, J.A. (1987) Fluorescence resonance energy transfer measurements of distances in actin and myosin. A critical evaluation. *J. Muscle Res. Cell Motil.* **8**, 97-117
8. Miki, M., O'Donoghue, S.I., and dos Remedios, C.G. (1992) Structure of actin observed by fluorescence resonance energy transfer spectroscopy. *J. Muscle Res. Cell Motil.* **13**, 132-145
9. Tao, T., Gong, B-J., and Leavis, P.C. (1990) Calcium-induced movement of troponin-I relative to actin in skeletal muscle thin filaments. *Science* **247**, 1339-1341
10. Miki, M. (1990) Resonance energy transfer between points in a reconstituted skeletal muscle thin filament: A conformational change of the thin filament in response to a change in Ca^{2+} concentration. *Eur. J. Biochem.* **187**, 155-162
11. Miki, M. and Iio, T. (1993) Kinetics of structural changes of reconstituted skeletal muscle thin filaments observed by fluorescence resonance energy transfer. *J. Biol. Chem.* **268**, 7101-7106
12. Tao, T., Gowell, E., Strasburg, G.M., Gergely, J., and Leavis, P.C. (1989) Ca^{2+} dependence of the distance between Cys-98 of troponin C and Cys-133 of troponin I in the ternary troponin complex. *Biochemistry* **28**, 5902-5908
13. Zhao, X., Kobayashi, T., Malak, H., Gryczynski, I., Lakowicz, J., Wade, R., and Collins, J.H. (1995) Calcium-induced troponin flexibility revealed by distance distribution measurements between engineered sites. *J. Biol. Chem.* **270**, 15507-15514
14. Kabsch, W., Mannherz, H.G., Suck, D., Pai, E.F., and Holmes, K.C. (1990) Atomic structure of the actin: DNase I complex. *Nature* **347**, 37-44
15. Ojima, T. and Nishita, K. (1988) Separation of akazara scallop and rabbit troponin components by a single-step chromatography on CM-Toyopearl. *J. Biochem.* **104**, 9-11
16. Nonaka, M., Sakamoto, H., Toiguchi, S., Kawajiri, H., Soeda, T., and Motoki, M. (1992) Sodium caseinate and skim milk gels formed by incubation with microbial transglutaminase. *J. Food Sci.* **57**, 1214-1241
17. Kim, E., Motoki, M., Seguro, K., Muhlrad, A., and Reisler, E.

(1995) Conformational changes in subdomain 2 of G-actin; Fluorescence probing by dansyl ethylenediamine attached to Gln-41. *Biophys. J.* **69**, 2024-2032
18. Lehrer, S.S. and Kerwar, G. (1972) Intrinsic fluorescence of actin. *Biochemistry* **11**, 1211-1217
19. Weeds, A.G. and Pope, B. (1977) Studies on the chymotryptic digestion of myosin. Effects of divalent cations on proteolytic susceptibility. *J. Mol. Biol.* **111**, 129-157
20. Cummins, P. and Perry, S.V. (1973) The subunits and biological activity of polymorphic forms of tropomyosin. *Biochem. J.* **133**, 765-777
21. Ishiwata, S. and Fujime, S. (1972) Effect of calcium ions on the flexibility of reconstituted thin filaments of muscle studied by quasielastic scattering of laser light. *J. Mol. Biol.* **68**, 511-522
22. Grabarek, Z., Mabuchi, Y., and Gergely, J. (1995) Properties of troponin C acetylated at lysine residues. *Biochemistry* **34**, 11872-11881
23. Hiratsuka, T. and Uchida, K. (1973) Preparation and properties of 2′(or 3′)-*O*-(2,4,6-trinitrophenyl)adenosine 5′-triphosphate, an analog of adenosine triphosphate. *Biochim. Biophys. Acta* **320**, 635-647
24. Takashi, R. (1988) A novel actin label: a fluorescent probe at glutamine-41 and its consequences. *Biochemistry* **27**, 938-943
25. Lorand, L., Parameswaran, K.N., Velasco, P.T., Hsu, L.K.-H., and Siefring, G.E., Jr. (1983) New colored and fluorescent amine substrates for activated fibrin stabilizing factor (Factor XIIIa) and for transglutaminase. *Anal. Biochem.* **131**, 419-425
26. Lakowicz, J.R. (1983) *Principles of Fluorescence Spectroscopy*, Plenum Press, New York
27. Fairclough, R.H. and Cantor, C.R. (1978) The use of singlet-singlet energy transfer to study macromolecular assemblies. *Methods Enzymol.* **48**, 347-379
28. Scott, T.G., Spencer, R.D., Leonard, N.G., and Weber, G. (1970) Emission properties of NADH. Studies of fluorescence lifetimes and quantum efficiencies of NADH, AcPyADH, and simplified synthetic models. *J. Am. Chem. Soc.* **92**, 687-695
29. Dale, R.E., Eisinger, J., and Blumberg, W.E. (1979) Orientational freedom of molecular probes. Orientation factor in intramolecular energy transfer. *Biophys. J.* **26**, 161-194
30. Laemmli, U.K. (1970) Cleavage of structural proteins during the assembly of the head of bacteriophage T4. *Nature* **227**, 680-685
31. Tausky, H.H. and Shorr, E. (1953) A microcolorimetric method for the determination of inorganic phosphorus. *J. Biol. Chem.* **202**, 675-685
32. Grabarek, Z., Grabarek, J., Leavis, P.C., and Gergely, J. (1983) Cooperative binding to the Ca^{2+}-specific sites of troponin C in regulated actin and actomyosin. *J. Biol. Chem.* **258**, 14098-14102
33. Miki, M. (1987) The recovery of the polymerizability of Lys-61-labeled actin by the addition of phalloidin. *Eur. J. Biochem.* **164**, 229-235
34. Kasprzak, A.A., Takashi, R., and Morales, M.F. (1988) Orientation of the actin monomer in the F-actin filament: radial coordinate of glutamine-41 and effect of myosin subfragment-1 binding on the monomer orientation. *Biochemistry* **27**, 4512-4522
35. Stryer, L. (1978) Fluorescence energy transfer as a spectroscopic ruler. *Annu. Rev. Biochem.* **47**, 819-846
36. dos Remedios, C.G. and Moens, P.D.J. (1995) Fluorescence resonance energy transfer spectroscopy is a reliable "ruler" for measuring structural changes in proteins. Dispelling the problem of the unknown orientation factor. *J. Struct. Biol.* **115**, 175-185
37. Reinach, F.C., Farah, C.S., Monteiro, P.B., and Malnic, B. (1997) Structural interactions responsible for the assembly of the troponin complex on the muscle thin filament. *Cell Struct. Funct.* **22**, 219-223
38. Lorenz, M., Popp, D., and Holmes, K.C. (1993) Refinement of the F-actin model against x-ray fiber diffraction data by the use of a directed mutation algorithm. *J. Mol. Biol.* **234**, 826-836
39. Grabarek, Z. and Gergely, J. (1987) Location of the TnI binding site in the primary structure of actin. *Acta Biochim. Biophys. Hung.* **22**, 307-316
40. Milligan, R.A., Whittaker, M., and Safer, D. (1990) Molecular structure of F-actin and location of surface binding sites. *Nature* **348**, 217-221
41. Saeki, K., Sutoh, K., and Wakabayashi, T. (1996) Tropomyosin-binding site(s) on the *Dictyostelium* actin surface as identified by site-directed mutagenesis. *Biochemistry* **35**, 14465-14472
42. Bertrand, R., Chaussepied, P., Audemard, E., and Kassab, R. (1989) Functional characterization of skeletal F-actin labeled on the N-terminal segment of residues 1-28. *Eur. J. Biochem.* **181**, 745-754
43. Sutoh, K., Ando, M., Sutoh, K., and Toyoshima, Y.Y. (1991) Site-directed mutation of dictyostelium actin: disruption of a negative charge cluster at the N-terminus. *Proc. Natl. Acad. Sci. USA* **88**, 7711-7714